Distribution and characteristic of nitrite-dependent anaerobic methane oxidation in wastewater treatment plants and agriculture fields of northern China

Zhen Hu Corresp., [1] , **Ru Ma** [1]

[1] School of Environmental Science and Engineering, Shandong University, Jinan, China

Corresponding Author: Zhen Hu
Email address: huzhen885@sdu.edu.cn

Nitrite-dependent anaerobic methane oxidation (n-damo), performed by "*Candidatus* Methylomirabilis oxyfera", which is affiliated to NC10 phylum, is a recently discovered biological process. In this study, molecular biological techniques and potential n-damo activity batch experiments were conducted to identify the presence and diversity of *M. oxyfera* bacteria in paddy field, corn field, and wastewater treatment plant (WWTP) of northern China, as well as lab-scale n-damo enrichment culture. N-damo enrichment culture showed the highest abundance of 16S rRNA genes of *M. oxyfera* (1.07×10^{10} copies per gram of dry sediment), which was 4.1×10^{3} times higher than that in WWTP. The anaerobic methane oxidation rates were significantly correlated to the abundance of *M. oxyfera* bacteria and it reduced from 22.31±0.02 μmol CH_4 g^{-1} d^{-1} in n-damo enrichment culture to 1.61 ± 0.01 μmol CH_4 g^{-1} d^{-1} in WWTP. Sequencing analysis revealed that corn field had the highest operational taxonomic units (OUTs), which may be attributed to the high NO_X^--N content. And interestingly, the n-damo enrichment culture (WWTP sludge as inoculum) showed higher OUTs than WWTP, indicating that WWTP might not be suitable for the growth of *M. oxyfera* bacteria. This might be caused by the high ammonium concentration in WWTP, compared with the other three habitats. Given the abundance and diversity of *M. oxyfera* bacteria, it is believed that the paddy field and corn field have advantages over WWTP sludge as inoculum to enrich *M. oxyfera* bacteria.

Distribution and characteristic of nitrite-dependent anaerobic methane oxidation by comparative analysis of wastewater treatment plants and agriculture fields in northern China

Zhen Hu[a,*], Ru Ma [a]

[a] School of Environmental Science and Engineering, Shandong University, Jinan, Shandong, China.

Corresponding Author:

Zhen Hu

No. 27 Shanda South Road, Jinan, Shandong 250100,China

E-mail: huzhen885@sdu.edu.cn

10 **Introduction**

11 Methane (CH_4) and nitrous oxide (N_2O) are important greenhouse gases, accounting for around 20% and 7%
12 of global warming, respectively (Griggs & Noguer 2002; Knittel & Boetius 2009). It is reported that
13 anthropogenic activities, rather than natural sources, are the major sources of CH_4 and N_2O emissions (Cai
14 2012). Two of the most widely accepted anthropogenic sources are wastewater treatment plants (WWTP) and
15 agricultural fields (Foley et al. 2011; Liu et al. 2014a). In WWTP, enormous amount of CH_4 and N_2O would be
16 produced during the biological transformation of carbohydrates and nitrogenous compounds. Our previous on-
17 site measurement showed that the emission factors of CH_4 and N_2O in typical full-scale WWTP of northern
18 China were 11.3 g CH_4 person^{-1} yr^{-1} and 1.96 g N_2O person^{-1} yr^{-1}, respectively (Wang et al. 2011a; Wang et al.
19 2011b). Compared with WWTP, agricultural field is believed to be a more important GHGs source, mainly
20 because the widely usage of fertilizers. It is reported that agriculture field would contribute to 60% of N_2O and
21 50% of CH_4 emissions on a global scale (Montzka et al. 2011; Syakila & Kroeze 2011).

22 Anaerobic methane oxidation (AMO) is a recently discovered sink of methane on earth, with a consumption
23 rate of approximately 70–300 Tg CH_4 year^{-1} globally (Cui et al. 2015; Hu et al. 2011). Ettwig et al. (2010)
24 revealed that nitrite-dependent anaerobic methane oxidation (n-damo), which was performed by "*Candidatus*
25 Methylomirabilis oxyfera" (*M. oxyfera*) affiliated with the NC10 phylum, was the main path of AOM process.

Since n-damo process established a unique relationship between carbon cycle and nitrogen cycle (Raghoebarsing et al. 2006), it was believed to be a promising method to minimize greenhouse gases emissions through converting CH_4 and N_2O to CO_2 and N_2.

Presently, many researchers are enthusiastic about investigating the distribution *of M. oxyfera* bacteria in natural environment, and the presence of *M. oxyfera* bacteria have been verified in freshwater lakes (Liu et al. 2014b), paddy soil (Wang et al. 2012), marine sediments (Chen et al. 2014), wetlands (Hu et al. 2014b), and etc. In addition, enrichment of *M. oxyfera* have been successfully conducted by using various inoculums, including freshwater sediment (Raghoebarsing et al. 2006), sewage treatment sludge (Luesken et al. 2011a), ditch sediments (Ettwig et al. 2009) and paddy soil (Shen et al. 2014a; Wang et al. 2012). However, to date, information about distribution *of M. oxyfera* bacteria in environment of northern China is still lacking. Furthermore, although He et al. (2014) found that inoculum sources had significant effect on enrichment of *M. oxyfera* bacteria, and proved that paddy soil was the optimal inoculum, intensive study on inoculum sources from the perspective of microorganism is absence.

In this study, the diversity and abundance of *M. oxyfera* bacteria in four different sites of northern China, i.e., paddy field, corn field, n-damo enrichment culture and WWTP, were investigated through molecular biology analyses. Comparative analysis of environmental features and *M. oxyfera* bacteria activity was conducted to reveal the characteristics of *M. oxyfera* bacteria, and optimal inoculum for enrichment of *M.*

43 *oxyfera* bacteria was proposed.

44 **Materials and methods**

45 ***Site description and sample collection***

46 Non-flooded paddy field with rice reaping once per year (PF) and corn field with maize-wheat rotation for over
47 50 years (CF), both of which are typical agricultural type of northern China, were selected as agricultural field
48 sample sites. PF cores and CF cores were collected by mixing three locations (5m distance) at the 50cm-60cm
49 depth, according to the previously described methods (Hu et al. 2014b). Sludge from anaerobic tank of local
50 WWTP (Everbright Water, Jinan China) (WS), and lab-scale Upflow Anaerobic Sludge Bed reactor (UASB)
51 aiming at enrichment of *M.oxyfera* bacteria (EC), were selected as WWTP samples. The sample collection was
52 conducted in October, 2015, and the environmental characteristics of each sample sites were listed in Table 1.
53 All collected samples were placed in hermetic containers and immediately transported to the laboratory
54 within 4h. Subsequently, the collected samples were equally divided into three parts. The first part was placed
55 in the incubator to measure the potential n-damo rates, the second parts was stored in refrigerator at 4℃ for
56 analysis of physicochemical parameters, and the last part was stored in refrigerator at -20℃ for further
57 microbiological analysis.

58 **Table 1.** Environmental characteristics of the collected sample sites.

Sample sites	Geographic coordinates	Temperature (℃)	pH	Ammonium (mg N/kg dry sed)	Nitrite (mg N/kg dry sed)	Nitrate (mg N/kg dry sed)	Salinity (‰)
PF	N36° 41', E116° 54'	17	7.3	10.34	0.75	26.97	1.8
CF	N37° 44', E115° 40'	15	7.0	2.627	0.37	46.44	1.1
EC	N36° 40', E117° 03'	32	7.0	0.125	14117.65	941.18	1.2
WS	N36° 42', E117° 02'	22	7.6	815.88	127.19	735.29	2.1

59 ***Physicochemical parameters analysis***

60 Soil samples were extracted with 1M KCl and the concentrations of ammonium, nitrite and nitrate were

61 measured as described by Ryan et al. (2007). Soil pH was measured at a soil/water ratio of 1:2.5 using a pH

62 analyzer (HQ30d 53LEDTM, HACH, USA) (Wang et al. 2012). The temperature and salinity of soil was

63 measured in *situ* using a HI98331 soil electrical conductivity meter (HANNA, Shanghai).

64 Concentrations of ammonium, nitrite and nitrate in water samples were analyzed according to standard

65 method (APHA 2005). Water temperature, pH and salinity were measured in *situ* using a pH and salinity

66 analyzer (DDBJ-350, Leici, Shanghai). And CH_4 concentration was analyzed using a gas chromatograph

67 equipped with flame ionization detector (FID–GC) (7890B, GC system, Agilent Technologies).

Potential n-damo activity batch experiment

All the samples were washed three times with anaerobic water to remove the residual NO_x^- (NO_2^- and NO_3^-) and organic compounds, and then were transferred to 1L Ar-flushed glass bottles. The soil slurries were pre-incubated under anoxic conditions for at least 48 h to recover the microbial activity, and then flushed with Ar gas again before the measurement of potential n-damo activity. Two treatment groups were conducted subsequently: (a) CH_4 (blank group, CH_4 at 99%), (b) CH_4+NO_2^-(experimental group). The initial CH_4 concentrations in both blank and experimental groups were around 1.00 mmol L^{-1}, and the initial concentrations of NO_2^- in the experimental groups were around 0.35 mmol NO_2^- L^{-1}. The variation of CH_4 and NO_2^- concentrations were determined at intervals of 6 hours. The potential methane oxidation rates and the ratio of CH_4/NO_2^- were evaluated by linear regression of the concentrations of CH_4 and NO_2^- in the experimental groups.

Fluorescence in situ hybridization (FISH)

Approximately 0.3g of collected samples were washed in phosphate-buffered saline (PBS; 10 mM Na_2HPO_4/NaH_2PO_4 pH 7.5 and 130 mM NaCl) and fixed with 4% (w/v) paraformaldehyde in PBS for 3h under 4℃. After incubation, the sediment (fixed biomass) was washed with PBS and then stored in mixture (1ml) of

ethanol and PBS (1×) at −20 ℃ until analysis.

Bacterial probe S-*-DBACT-1027-a-A-18 (5'-TCTCCACGCTCCCTTGCG-3') (Cy3, red), specific for bacteria affiliated with the NC10 phylum were used in this study (Raghoebarsing et al. 2006); and a mixture of EUB I-III (FITC, green) was used for the detection of total bacteria (Daims et al. 1999). Fixed biomass (10 μl) was spotted on microscopic slides circles and then dehydrated subsequently with 50%, 80%, and 98% of ethanol for 3min each. The probes were hybridized for 2 h at 46 °C in hybridization buffer (5M NaCl, 1M Tris/HCl pH 8.0, 10% sodium dodecyl sulfate) and 40% formamide. Hybridized samples were washed with hybridization leachate at 48℃ and then added with the fluorescence decay resistance agent. Fluorescence microscope (Olympus BX53, Japan) was used to observe the prepared slides and the picture was disposed with software Image-Pro Plus 6.0.

DNA extraction and PCR amplification

Total DNA was extracted using Power Soil DNA kit (Mo Bio Laboratories, Carlsbad, CA) according to the manufacturer's instructions. The DNA concentration was measured at 260nm with a Nano-drop spectrophotometer (Nano-Drop Technologies, USA).

To understand the biodiversity of *M. oxyfera* bacteria, 16S rRNA gene and *pmoA* gene of *M. oxyfera* bacteria were amplified using nested PCR protocols, as previously described (Hu et al. 2014b; Luesken et al.

2011b). For 16S rRNA gene amplification, specific forward primer 202F (Ettwig et al. 2009) and general bacterial reverse primer 1545R (Juretschko et al. 1998) were used for the first round, NC10 specific primers qP1F and qP2R (Ettwig et al. 2009) were performed for the second round. For *pmoA* gene amplification, the forward primer A189_b and the reverse primer cmo682 (Luesken et al. 2011b) were used firstly, and the primer cmo182 and cmo568 were used in the following nested PCR (Luesken et al. 2011b). The detailed information of nested PCR is shown in Table S1.

Quantitative Real-Time PCR (qPCR)

M. oxyfera 16S rRNA gene copy numbers in all four samples were calculated in triplicate, using the fluorescent dye SYBR Green, based on LightCycler480 with Sequence Detection Software v1.4 (Applied Biosystems, USA). The quantitative PCR of 16S rRNA gene was determined using the primers qp1R-qp1F (Ettwig et al. 2009) with 20-μL system. Each system was comprised of 10 μL of Power SYBR Green PCR Master Mix (Applied BioSystems), 1 μL of template DNA (5–20 ng μL^{-1}), 0.4 μL of each primer and 8.2 μL of ddH_2O. Detailed information is exhibited in Table S1. DNA plasmid containing the target genes was continuously diluted 10 times in order to obtain the standard curve. The standard curve showed excellent correlation between the DNA template concentration and the crossing point with high coefficients of determination (R^2>0.97).

115 ***Sequencing and phylogenetic analyses***

116 Nucleotide sequences of *M.oxyfera* were measured by 454 high-throughput sequencing (16S rRNA gene) and
117 Illumina MiSeq sequencing (*pmoA* gene), accomplished by Shanghai Personalbio-pharm Technology Co., Ltd
118 (Shanghai, China). Sequences were clustered into operational taxonomic unites (OTUs) by UCLUST (Edgar et
119 al. 2011). Chao1 richness estimator, ACE estimator, Simpson diversity and Good's coverage were calculated
120 in Mothur analysis (http://www.mothur.org). Sequences analyses were operated by BLAST searching to obtain
121 related sequences (>90% similarity) from NCBI (http://www.ncbi.nlm.nih.gov/GenBank/) and sequence
122 similarity was performed in Clustal W version 2.1. Phylogenetic trees were established with MEGA 4.0
123 software (Tamura et al. 2007) using the neighbor-joining method with *p* distance correction and a 1,000-
124 replicate bootstrap value (Hu et al. 2014a).

125 ***Nucleotide sequence accession numbers***

126 Sequences obtained from these samples were divided into 16S rRNA and *pmoA* of *M. oxyfera*, and were
127 submitted to GenBank under accession numbers KX153190-KX153201 and KX153202-KX153210,
128 respectively.

129 **Results**

130 ***Physicochemical Characteristics of the Sample Sites***

131 Significant differences in physicochemical characteristics among different environmental samples were
132 observed in present study. The peak NH_4^+-N content was detected in WS (815.88 mg N kg^{-1} dry sediment),
133 which was over 80-folds higher than that in the other three sample sites. And highest NO_2^- -N content was
134 observed in the EC (14120 mg N kg^{-1} dry sediment), while NO_2^- -N content in the other three sample site
135 varied form 0.37-127.19 mg N kg^{-1} dry sediment. Because of it high NO_2^- content, the highest NO_x^--N content
136 was also observed in the EC, which was beyond 17-fold higher than that of the other three sample sites. In
137 addition, compared with published research conducted in paddy field, where NO_X^--N content was around 1.4
138 mg N kg^{-1} dry sediment (Shen et al. 2014a), higher NO_X^--N content in the agriculture field (PF and CF) of
139 northern China were observed in this study, manly caused by difference in farming methods .

140 ***Abundance of M.oxyfera bacteria***

141 FISH analysis was used to investigate the spatial distribution and relative quantification of *M. oxyfera* bacteria
142 compared to total bacteria. As shown in Fig. 1, *M. oxyfera* bacteria were observed in all four sample sites
143 (represented by red color), and the proportion of *M. oxyfera* bacteria to total bacteria followed the order of
144 EC>PF>CF>WS. Notably, compared with total bacteria, *M.oxyfera* bacteria in the enrichment culture took up

over 50%，which was in consistence with that reported in other enrichment culture (He et al. 2014; Hu et al. 2014a; Kampman et al. 2014).

To further accurately quantify the abundance of *M. oxyfera* bacteria, qPCR analysis was conducted and significant difference was also observed in different sampling sites. The abundance of *M. oxyfera* bacteria were $7.28\pm0.8\times10^{7}$,$1.55\pm0.3\times10^{7}$, $1.07\pm0.3\times10^{10}$, $2.61\pm0.1\times10^{6}$ copies per gram of dry sediment in PF, CF, EC and WS, respectively (Fig.2). This order was in agreement with result of FISH analysis.

Fig. 1 *FISH image of the collected samples. The M. oxyfera bacteria was hybridized with probe S-*-DBACT-1027-a-A-18(Cy3, red) and total bacteria was hybridized with probes EUB I-III (FITC, green). a&e, PF; b&f, CF; c&g, EC, d&h, WS. The scale bar indicates 100 μm.*

Fig. 2 *The abundance of M. oxyfera bacteria in different sample sites.*

Potential Rates of n-damo Activity

In order to estimate the activity of *M. oxyfera* bacteria, two groups of experiments were operated using the collected samples, and the results are shown in Fig. 3. In experimental groups amended with CH_4 and NO_2^-, dramatic decline in CH_4 concentration were observed compared with the blank groups, indicating that CH_4 oxidation was propelled by NO_2^- reduction under anoxic conditions. The detected anaerobic methane oxidizing rates were 3.90±0.05, 2.58±0.08, 22.31±0.02 and 1.61±0.01 μmol CH_4 g^{-1} d^{-1} in PF, CF, EC and WS,

162 respectively. The stoichiometric ratio for methane to nitrite, calculated through the curve fitting method, were
163 3:5.7 for PF, 3:4.6 for CF, 3:6.9 for EC, and 3:3.2 for WS. The value of n-damo enrichment culture was the
164 closest to the theoretical stoichiometric ratio, which was 3:8 (Ettwig et al. 2010).

165

166 ***Fig. 3*** *The consumption rates of methane and nitrite in the paddy field (a), corn field (b), n-damo enrichment culture (c), WWTP*
167 *(d).*

168 ***Sequencing analysis of M. oxyfera bacteria 16S rRNA gene***

169 In order to estimate the distribution and composition of *M. oxyfera* bacteria, 454 high-throughput sequencing
170 analysis of 16S rRNA gene was conducted. Raw reads obtained from four libraries ranged from 11017 to
171 14814 and the good coverage values varied from 86.48% to 94.70% (Table S2), indicating that these sequences
172 were enough to analyze the microbial communities. The number of OTUs, Chao1 estimator, ACE estimator,
173 Shannon index and Simpson index based on 97% of the similar level were calculated (Table S2) to estimate
174 the community diversity.

175 The composition of bacteria community in four samples was described at the phylum level (Fig. S1). Some
176 sequences that could not be divided into any known group were classified into others. The first 7 phyla
177 obtained in four sample sites were *NC10*, *Acido*bacteria, *Armatimonadetes*, *Firmicutes*, *Proteo*bacteria,
178 *Nitrospirae*, *Verrucomicrobia*. *NC10, Acido*bacteria and *Armatimonadetes* were recognized as dominant phyla

179 since them accounting for 93.25% to 99.14% of total bacteria in all samples. For the better understanding of
180 the diversity of *M. oxyfera* bacteria, phylogenetic tree based on selecting all the sequences related to
181 *Candidatus* 'Methylomirabilis oxyfera' (similarities to *M. oxyfera* >90 %) was constructed and is shown in
182 Fig. 4. Sequences of *M. oxyfera* bacteria 16S rRNA gene were grouped into two groups according to Ettwig et
183 al.(2009) Sequences of group A, which were obtained from PF, CF, EC and WS, showed identity of 94.84-
184 99.31%, 94.20-99.17%, 94.47-99.31%, and 94.16-99.31% to the 16S rRNA gene of *M. oxyfera* bacteria,
185 respectively. Sequences of group B, acquired from the EC and PF, showed identity of 89.15-92.86% to the 16S
186 rRNA gene of *M. oxyfera* bacteria.
187
188 ***Fig. 4*** *Phylogenetic tree showing the phylogenetic affiliations of M. oxyfera bacteria 16S rRNA sequences in different sample*
189 *sites by neighbor-joining method. Bootstrap values were 1,000 replicates and the scale bar represents 2% of the sequence*
190 *divergence.*

191 ***Sequencing analysis of M. oxyfera bacteria pmoA gene***

192 The Illumina MiSeq sequencing analysis was used to detect the *pmo*A genes of *M. oxyfera* bacteria on a
193 functional level. Raw reads obtained from four libraries ranged from 63,186 to 96,276 and good's coverage
194 varied from 93.91 to 98.13%, indicating that the obtained sequences were able to confirm the bacteria
195 community structure on a functional level. The number of OTUs, Chao1 estimator, ACE estimator, Shannon

196 index and Simpson index based on 97% of the similar level were shown in Table S2.

197 The sequences, which were similar to the *pmo*A gene of *M. oxyfera*, were obtained to construct phylogenetic

198 tree, as shown in Fig. 5. Sequences recovered from PF, CF, EC and WS showed 89.76-91.4%, 90.3-92.7%,

199 89.8-91.4%, 90.3-91.4% of similarity to the *pmo*A gene of *M. oxyfera* bacteria, respectively.

200

201 ***Fig. 5*** *Neighbor-joining phylogenetic tree showing the phylogenetic affiliations of M. oxyfera bacteria pmoA gene sequences in*

202 *different sample sites. Bootstrap values were 1,000 replicates and the scale bar represents 5% of the sequence divergence.*

203

204 **Discussion**

205 In this study, PF, CF, EC and WS in northern China, as the previously overlooked sites, were selected to

206 investigate the presence and characteristics of n-damo process. Results showed that EC had the highest

207 potential n-damo rate, and it also had the highest abundance of *M. oxyfera* bacteria. Correlation analysis

208 showed that the potential n-damo rates and the abundance of *M. oxyfera* followed the same descending order,

209 i.e., EC>PF>CF>WS, indicating that the two indexes were significantly correlated with each other. This also

210 explained why the measured potential n-damo rate in EC of the present study was higher than that reported in

211 other n-damo enrichment culture (He et al. 2014). The abundance of *M. oxyfera* bacteria in the present study

212 was over 20 times higher than that reported by He et al. (2014), which was only $5.0\pm0.4\times10^8$ copies g^{-1} dry

213 weight.

214 WWTP showed lower abundance of *M. oxyfera* bacteria than the other three sample sites, mainly because
215 the high NH_4^+ content in WWTP might enhance the competition between Anammox bacteria and *M. oxyfera*
216 bacteria for nitrite. Winkler et al. (2015) found that the anammox bacteria had an advantage over *M. oxyfera*
217 bacteria for nitrite in the presence of excess ammonium. What is more interesting, although WS was used as
218 initial inoculum for EC, the abundance of *M. oxyfera* bacteria in EC was over 4×10^3 times higher than that in
219 WS. This was attributed to the high NO_2^- content during the enrichment period in EC. It was reported that the
220 nitrite affinity constant of was 0.6 g NO_2^-- Nm^{-3}, indicating that high NO_2^- content was more beneficial for the
221 growth of *M .oxyfera* bacteria (Winkler et al. 2015).

222 The diversity of *M. oxyfera* bacteria was determined by 16S rRNA gene sequencing analysis. Group A of
223 *M. oxyfera* bacteria, which were the dominant bacteria responsible for conducting the n-damo process (Ettwig
224 et al. 2009; Hu et al. 2009; Luesken et al. 2011a), were obtained in all four sample sites, whereas the group B
225 members were primarily recovered from EC and PF. This result indicated that the community structure of *M.*
226 *oxyfera* in WWTP was changed after cultivation. In addition, after cultivation, increase of 3 OTUs was
227 observed from WWTP to n-damo EC in the present study. This was mainly due to the optimum environment
228 of the enrichment culture, e.g., the combination of low NH_4^+ and high NO_2^- contents, which was favorable for
229 the growth of *M. oxyfera* bacteria. Meanwhile, compared with WS, PF and CF were believed to be better

inoculum to enrich *M. oxyfera* bacteria due to their higher abundance and diversity of *M. oxyfera* bacteria. Furthermore, the diversity and abundance of *M. oxyfera* in CF were not only higher than that detected in PF in present study, but also higher than the reported value in paddy field of Hangzhou, southern China (Shen et al. 2014a). This was attributed to the high NO_X^--N content observed in the soil cores in CF of the present study, which was over 27 times higher than that examined in Hangzhou.

The diversity of *M.oxyfera* bacteria *pmo*A gene observed in agriculture fields (PF and CF) were 6 and 7 OTUs, respectively, which were higher than most of the previously examined freshwater habitats, including wetland (Hu et al. 2014b; Shen et al. 2015), paddy soil (Shen et al. 2014a) and lake (Deutzmann & Schink 2011). And higher *M.oxyfera* bacteria diversity were observed in Jiaojiang Estuary (Shen et al. 2014b) and South China Sea (Chen et al. 2014). This indicated that salinity played a very import role in the diversity of *M. oxyfera* bacteria *pmoA* gene, which was consistence with the research findings of Chen et al. (2014). In addition, the n-damo *pmo*A gene sequences obtained from four sample sites was mainly grouped within the Yellow River Estuary after phylogeny reconstruction. Since all four sampling sites in the present study were located inside the Yellow River basin, particularly the PF, which was perennially irrigated with the water from Yellow River, indicating that the diversity of *M. oxyfera* bacteria might be related to geographical regions. However, further research and more direct evidence are needed to get this conclusion.

In conclusion, the present study further expanded our knowledge on the distribution of *M. oxyfera* bacteria

247 in wastewater treatment plants and agriculture fields of northern China. Comparative analysis showed that low
248 NH_4^+ and high NO_2^- contents would benefit the growth of *M. oxyfera* bacteria, and sample site with higher
249 abundance of *M. oxyfera* bacteria showed higher potential n-damo activity rate. Both paddy field and corn field
250 were believed to be optimum inoculum for the enrichment of *M. oxyfera* bacteria, due to their higher
251 abundance and diversity of *M. oxyfera* bacteria than that in WWTP. In addition, the diversity of *M. oxyfera*
252 bacteria was influenced by salinity, and might be related to geographical regions.

253 **Ethical Statement** This article does not contain any studies with human participants or animals performed
254 by any of the authors.

255 **Acknowledgments**

256 This study was funded by National Natural Science Foundation of China (No. 21307076), Fundamental
257 Research Funds of Shandong University (No. 2014TB003). And it was also supported by the AMIS (Fate and
258 Impact of Atmospheric Pollutants) project funded by the European Union, under the Marie Curie Actions
259 IRSES (International Research Staff Exchange Scheme), within the Seventh Framework Programme FP7-
260 PEOPLE-2011-IRSES. Sincere thanks to Dr. Hai Liu at Stanford University for his careful proof-reading of
261 this manuscript.

262

263 **References**

264 APHA. 2005. Standard methods for the examination of water and wastewater. *American Public Health*
265 *Association (APHA): Washington, DC, USA*.

266 Cai Z. 2012. Greenhouse gas budget for terrestrial ecosystems in China. *Science China Earth Sciences* 55:173-
267 182. 10.1007/s11430-011-4309-8

268 Chen J, Jiang X-W, and Gu J-D. 2014. Existence of Novel Phylotypes of Nitrite-Dependent Anaerobic
269 Methane-Oxidizing Bacteria in Surface and Subsurface Sediments of the South China Sea.
270 *Geomicrobiology Journal* 32:1-10. 10.1080/01490451.2014.917742

271 Cui M, Ma A, Qi H, Zhuang X, and Zhuang G. 2015. Anaerobic oxidation of methane: an "active" microbial
272 process. *MicrobiologyOpen* 4:1-11. 10.1002/mbo3.232

273 Daims H, Brühl A, Amann R, Schleifer K-H, and Wagner M. 1999. The Domain-specific Probe EUB338 is
274 Insufficient for the Detection of all Bacteria: Development and Evaluation of a more Comprehensive
275 Probe Set. *Systematic and Applied Microbiology* 22:434-444. 10.1016/s0723-2020(99)80053-8

276 Deutzmann JS, and Schink B. 2011. Anaerobic oxidation of methane in sediments of Lake Constance, an
277 oligotrophic freshwater lake. Appl Environ Microbiol. p 4429-4436.

278 Edgar RC, Haas BJ, Clemente JC, Quince C, and Knight R. 2011. UCHIME improves sensitivity and speed of
279 chimera detection. *Bioinformatics* 27:2194-2200.

280 Ettwig KF, Butler MK, Le Paslier D, Pelletier E, Mangenot S, Kuypers MM, Schreiber F, Dutilh BE, Zedelius
281 J, de Beer D, Gloerich J, Wessels HJ, van Alen T, Luesken F, Wu ML, van de Pas-Schoonen KT, Op
282 den Camp HJ, Janssen-Megens EM, Francoijs KJ, Stunnenberg H, Weissenbach J, Jetten MS, and

283 Strous M. 2010. Nitrite-driven anaerobic methane oxidation by oxygenic bacteria. *Nature* 464:543-
284 548. 10.1038/nature08883
285 Ettwig KF, van Alen T, van de Pas-Schoonen KT, Jetten MSM, and Strous M. 2009. Enrichment and
286 Molecular Detection of Denitrifying Methanotrophic Bacteria of the NC10 Phylum. *Applied and*
287 *Environmental Microbiology* 75:3656-3662. 10.1128/aem.00067-09
288 Foley JA, Ramankutty N, Brauman KA, Cassidy ES, Gerber JS, Johnston M, Mueller ND, O'Connell C, Ray
289 DK, West PC, Balzer C, Bennett EM, Carpenter SR, Hill J, Monfreda C, Polasky S, Rockstrom J,
290 Sheehan J, Siebert S, Tilman D, and Zaks DP. 2011. Solutions for a cultivated planet. *Nature* 478:337-
291 342. 10.1038/nature10452
292 Griggs DJ, and Noguer M. 2002. Climate change 2001: the scientific basis. Contribution of working group I to
293 the third assessment report of the intergovernmental panel on climate change. *Weather* 57:267-269.
294 He Z, Cai C, Shen L, Lou L, Zheng P, Xu X, and Hu B. 2014. Effect of inoculum sources on the enrichment of
295 nitrite-dependent anaerobic methane-oxidizing bacteria. *Appl Microbiol Biotechnol* 99:939-946.
296 10.1007/s00253-014-6033-8
297 Hu B, He Z, Geng S, Cai C, Lou L, Zheng P, and Xu X. 2014a. Cultivation of nitrite-dependent anaerobic
298 methane-oxidizing bacteria: impact of reactor configuration. *Appl Microbiol Biotechnol* 98:7983-7991.
299 10.1007/s00253-014-5835-z
300 Hu BL, Shen LD, Lian X, Zhu Q, Liu S, Huang Q, He ZF, Geng S, Cheng DQ, Lou LP, Xu XY, Zheng P, and
301 He YF. 2014b. Evidence for nitrite-dependent anaerobic methane oxidation as a previously
302 overlooked microbial methane sink in wetlands. *Proc Natl Acad Sci U S A* 111:4495-4500.
303 10.1073/pnas.1318393111
304 Hu S, Zeng RJ, Burow LC, Lant P, Keller J, and Yuan Z. 2009. Enrichment of denitrifying anaerobic methane

oxidizing microorganisms. *Environmental Microbiology Reports* 1:377-384.

Hu S, Zeng RJ, Keller J, Lant PA, and Yuan Z. 2011. Effect of nitrate and nitrite on the selection of microorganisms in the denitrifying anaerobic methane oxidation process. *Environ Microbiol Rep* 3:315-319. 10.1111/j.1758-2229.2010.00227.x

Juretschko S, Timmermann G, Schmid M, Schleifer K-H, Pommerening-Röser A, Koops H-P, and Wagner M. 1998. Combined molecular and conventional analyses of nitrifying bacterium diversity in activated sludge: Nitrosococcus mobilis and Nitrospira-like bacteria as dominant populations. *Applied and environmental microbiology* 64:3042-3051.

Kampman C, Temmink H, Hendrickx TLG, Zeeman G, and Buisman CJN. 2014. Enrichment of denitrifying methanotrophic bacteria from municipal wastewater sludge in a membrane bioreactor at 20°C. *Journal of Hazardous Materials* 274:428-435. 10.1016/j.jhazmat.2014.04.031

Knittel K, and Boetius A. 2009. Anaerobic Oxidation of Methane: Progress with an Unknown Process. *Annual Review of Microbiology*, 311-334.

Liu Y, Cheng X, Lun X, and Sun D. 2014a. CH4 emission and conversion from A2O and SBR processes in full-scale wastewater treatment plants. *Journal of Environmental Sciences* 26:224-230. http://dx.doi.org/10.1016/S1001-0742(13)60401-5

Liu Y, Zhang J, Zhao L, Li Y, Yang Y, and Xie S. 2014b. Aerobic and nitrite-dependent methane-oxidizing microorganisms in sediments of freshwater lakes on the Yunnan Plateau. *Appl Microbiol Biotechnol* 99:2371-2381. 10.1007/s00253-014-6141-5

Luesken FA, van Alen TA, van der Biezen E, Frijters C, Toonen G, Kampman C, Hendrickx TLG, Zeeman G, Temmink H, Strous M, Op den Camp HJM, and Jetten MSM. 2011a. Diversity and enrichment of nitrite-dependent anaerobic methane oxidizing bacteria from wastewater sludge. *Appl Microbiol*

Biotechnol 92:845-854. 10.1007/s00253-011-3361-9

Luesken FA, Zhu B, van Alen TA, Butler MK, Diaz MR, Song B, Op den Camp HJM, Jetten MSM, and Ettwig KF. 2011b. pmoA Primers for Detection of Anaerobic Methanotrophs. *Applied and Environmental Microbiology* 77:3877-3880. 10.1128/aem.02960-10

Montzka SA, Dlugokencky EJ, and Butler JH. 2011. Non-CO2 greenhouse gases and climate change. *Nature* 476:43-50. 10.1038/nature10322

Raghoebarsing AA, Pol A, van de Pas-Schoonen KT, Smolders AJ, Ettwig KF, Rijpstra WI, Schouten S, Damste JS, Op den Camp HJ, Jetten MS, and Strous M. 2006. A microbial consortium couples anaerobic methane oxidation to denitrification. *Nature* 440:918-921. 10.1038/nature04617

Ryan J, Estefan G, and Rashid A. 2007. *Soil and plant analysis laboratory manual*: ICARDA.

Shen L-d, Liu S, He Z-f, Lian X, Huang Q, He Y-f, Lou L-p, Xu X-y, Zheng P, and Hu B-l. 2015. Depth-specific distribution and importance of nitrite-dependent anaerobic ammonium and methane-oxidising bacteria in an urban wetland. *Soil Biology and Biochemistry* 83:43-51. http://dx.doi.org/10.1016/j.soilbio.2015.01.010

Shen L-d, Liu S, Huang Q, Lian X, He Z-f, Geng S, Jin R-c, He Y-f, Lou L-p, and Xu X-y. 2014a. Evidence for the cooccurrence of nitrite-dependent anaerobic ammonium and methane oxidation processes in a flooded paddy field. *Applied and environmental microbiology* 80:7611-7619.

Shen L-d, Qun Z, Shuai L, Ping D, Jiang-ning Z, Dong-qing C, Xiang-yang X, Ping Z, and Bao-lan H. 2014b. Molecular evidence for nitrite-dependent anaerobic methane-oxidising bacteria in the Jiaojiang Estuary of the East Sea (China). *Appl Microbiol Biotechnol* 98:5029-5038. 10.1007/s00253-014-5556-3

Syakila A, and Kroeze C. 2011. The global nitrous oxide budget revisited. *Greenhouse Gas Measurement and*

Management 1:17-26. 10.3763/ghgmm.2010.0007

Tamura K, Dudley J, Nei M, and Kumar S. 2007. MEGA4: molecular evolutionary genetics analysis (MEGA) software version 4.0. *Molecular biology and evolution* 24:1596-1599.

Wang J, Zhang J, Wang J, Qi P, Ren Y, and Hu Z. 2011a. Nitrous oxide emissions from a typical northern Chinese municipal wastewater treatment plant. *Desalination and Water Treatment* 32:145-152. 10.5004/dwt.2011.2691

Wang J, Zhang J, Xie H, Qi P, Ren Y, and Hu Z. 2011b. Methane emissions from a full-scale A/A/O wastewater treatment plant. *Bioresource Technology* 102:5479-5485. 10.1016/j.biortech.2010.10.090

Wang Y, Zhu G, Harhangi HR, Zhu B, Jetten MSM, Yin C, and Op den Camp HJM. 2012. Co-occurrence and distribution of nitrite-dependent anaerobic ammonium and methane-oxidizing bacteria in a paddy soil. *FEMS Microbiology Letters* 336:79-88. 10.1111/j.1574-6968.2012.02654.x

Winkler MKH, Ettwig KF, Vannecke TPW, Stultiens K, Bogdan A, Kartal B, and Volcke EIP. 2015. Modelling simultaneous anaerobic methane and ammonium removal in a granular sludge reactor. *Water Research* 73:323-331. http://dx.doi.org/10.1016/j.watres.2015.01.039

Figure 1(on next page)

FISH image of the collected samples.

Fig. 1- FISH image of the collected samples. The *M. oxyfera* bacteria was hybridized with probe S-*-DBACT-1027-a-A-18(Cy3, red) and total bacteria was hybridized with probes EUB I-III (FITC, green). a&e, PF; b&f, CF; c&g, EC, d&h, WS. The scale bar indicates 100 μm.

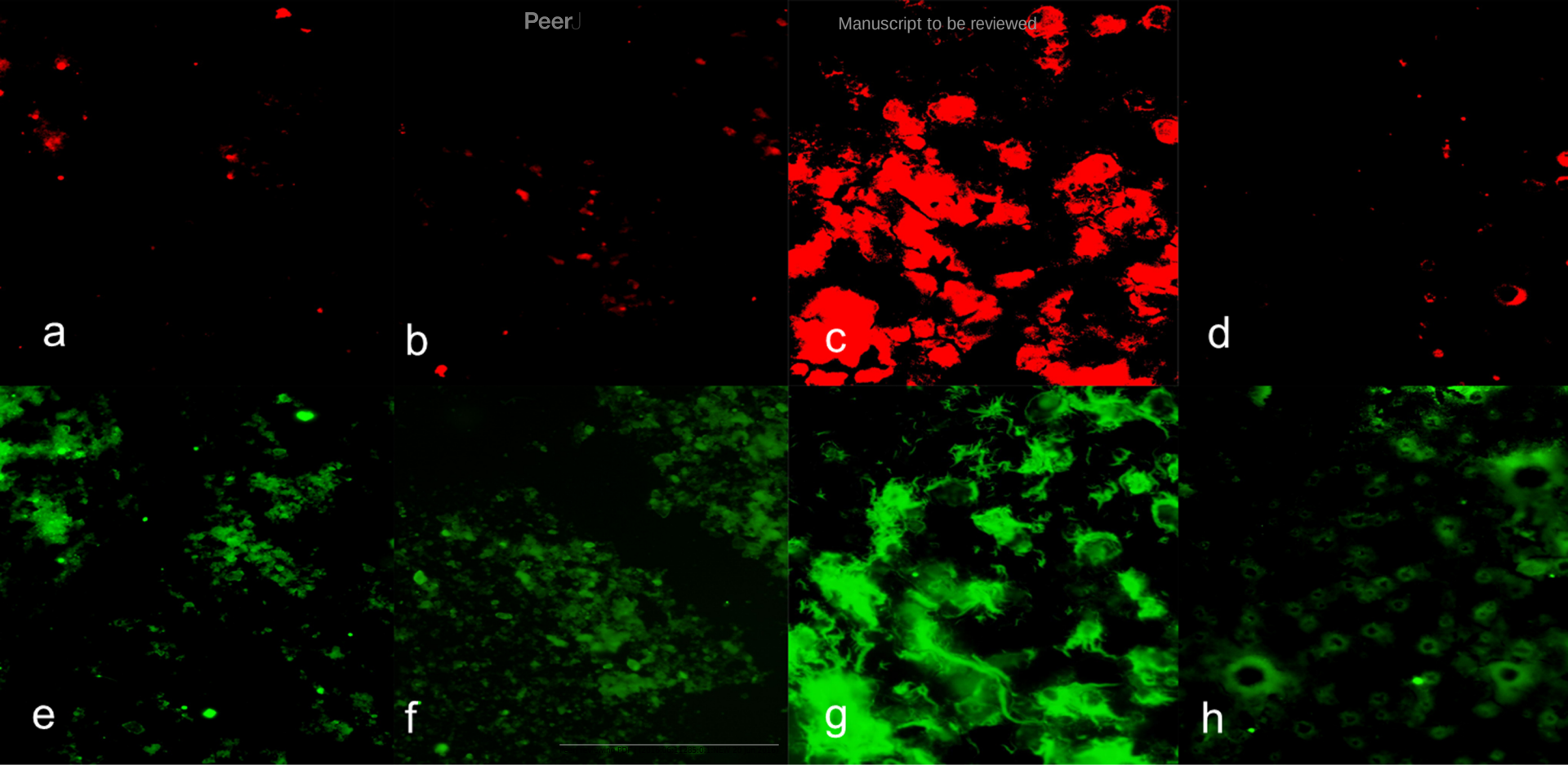

Figure 2(on next page)

Q-PCR Image of *M. oxyfera* bacteria

Fig. 2- The abundance of *M. oxyfera* bacteria 16S rRNA gene copy numbers of collected samples.

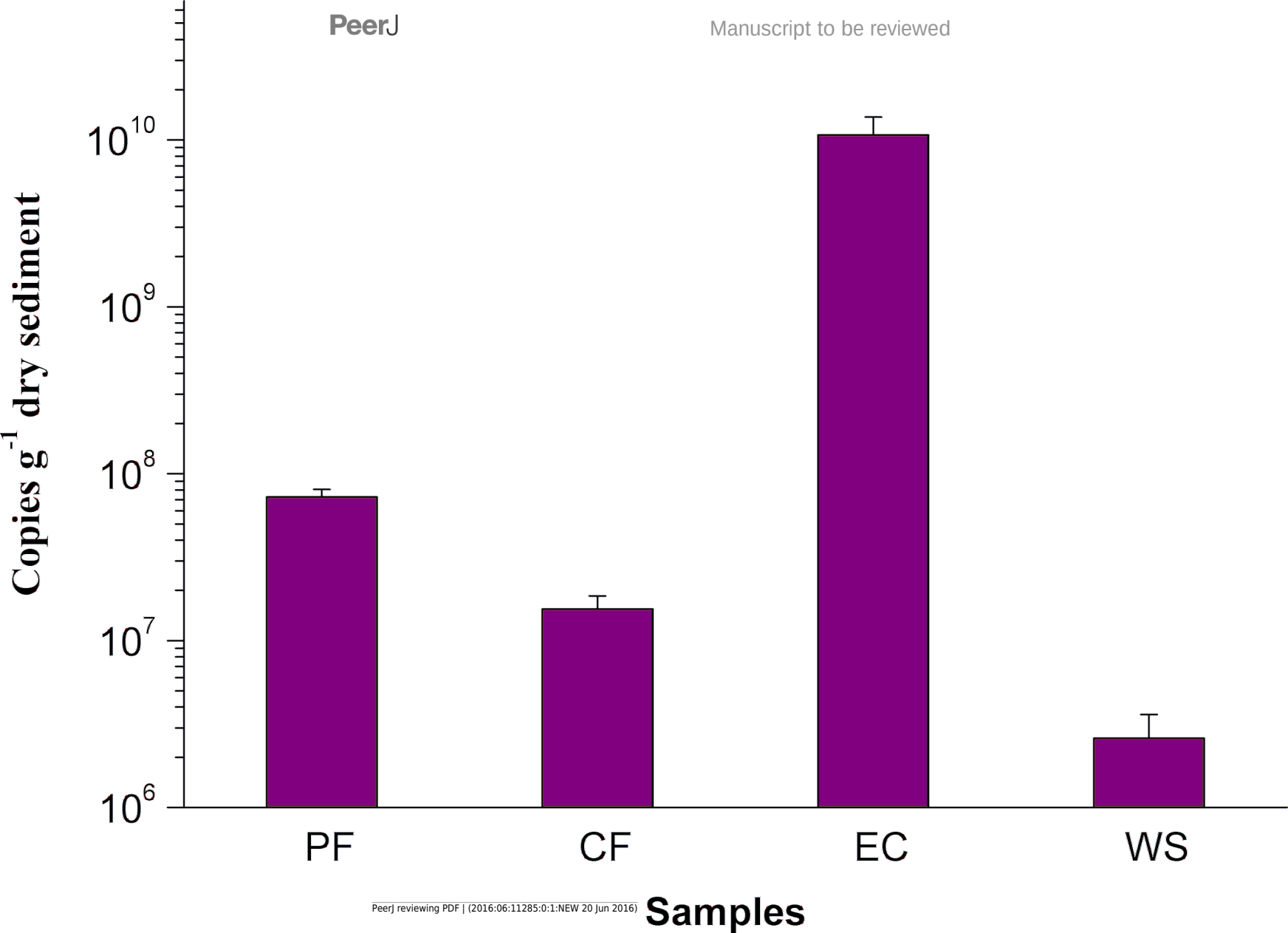
Copies g-1 dry sediment
10^10
10^9
10^8
10^7
10^6
PF
CF
EC
WS
Samples

Figure 3(on next page)

Image of batch test

Fig. 3 The consumption rates of methane and nitrite in the paddy field (a), corn field (b), n-damo enrichment culture (c), WWTP (d).

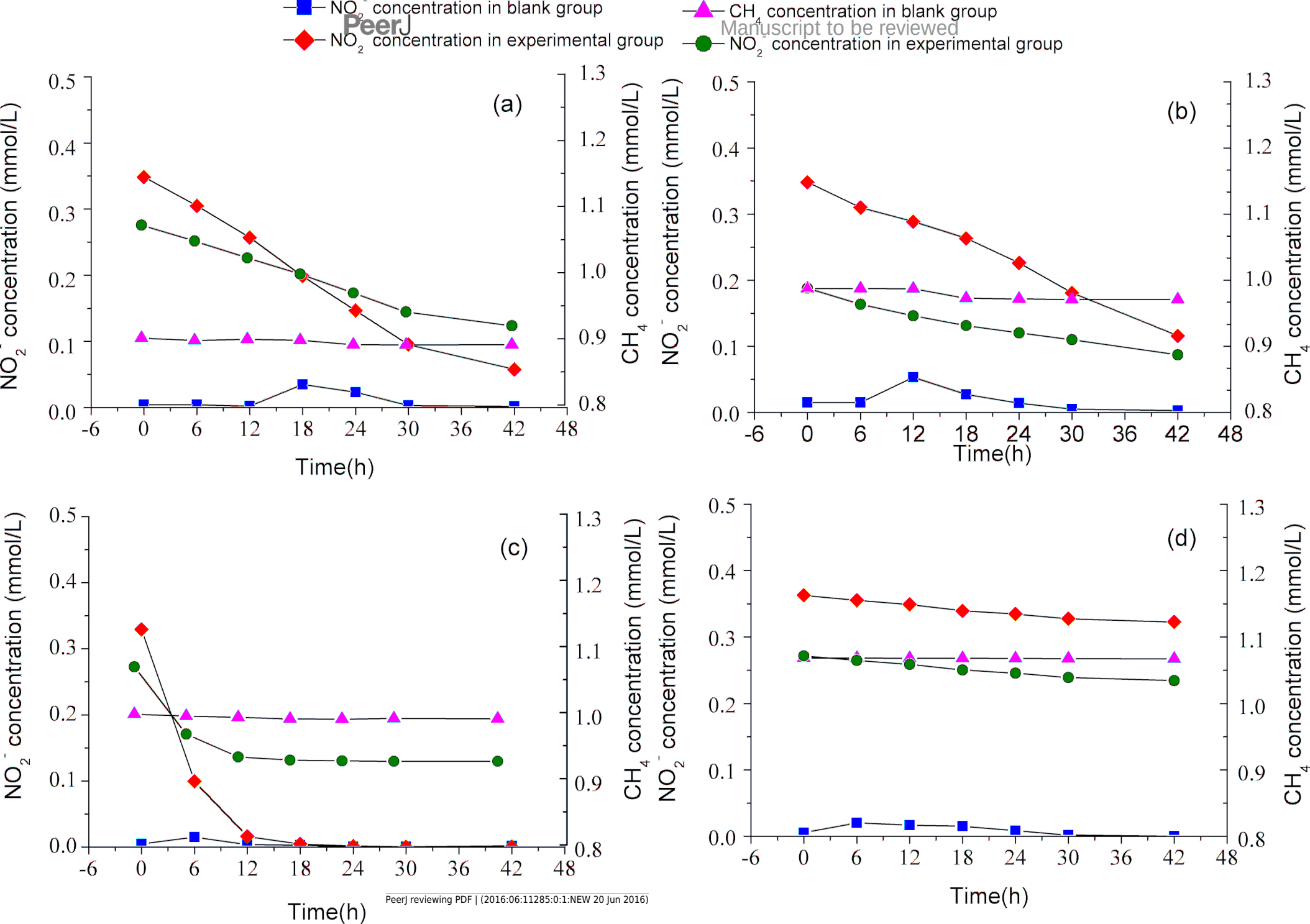

Figure 4(on next page)

Phylogenetic tree of *M. oxyfera* bacteria 16S rRNA sequences

Fig. 4 - Phylogenetic tree showing the phylogenetic affiliations of *M. oxyfera* bacteria 16S rRNA sequences in four samples by neighbor-joining method. Bootstrap values were 1,000 replicates and the scale bar represents 2% of the sequence divergence.

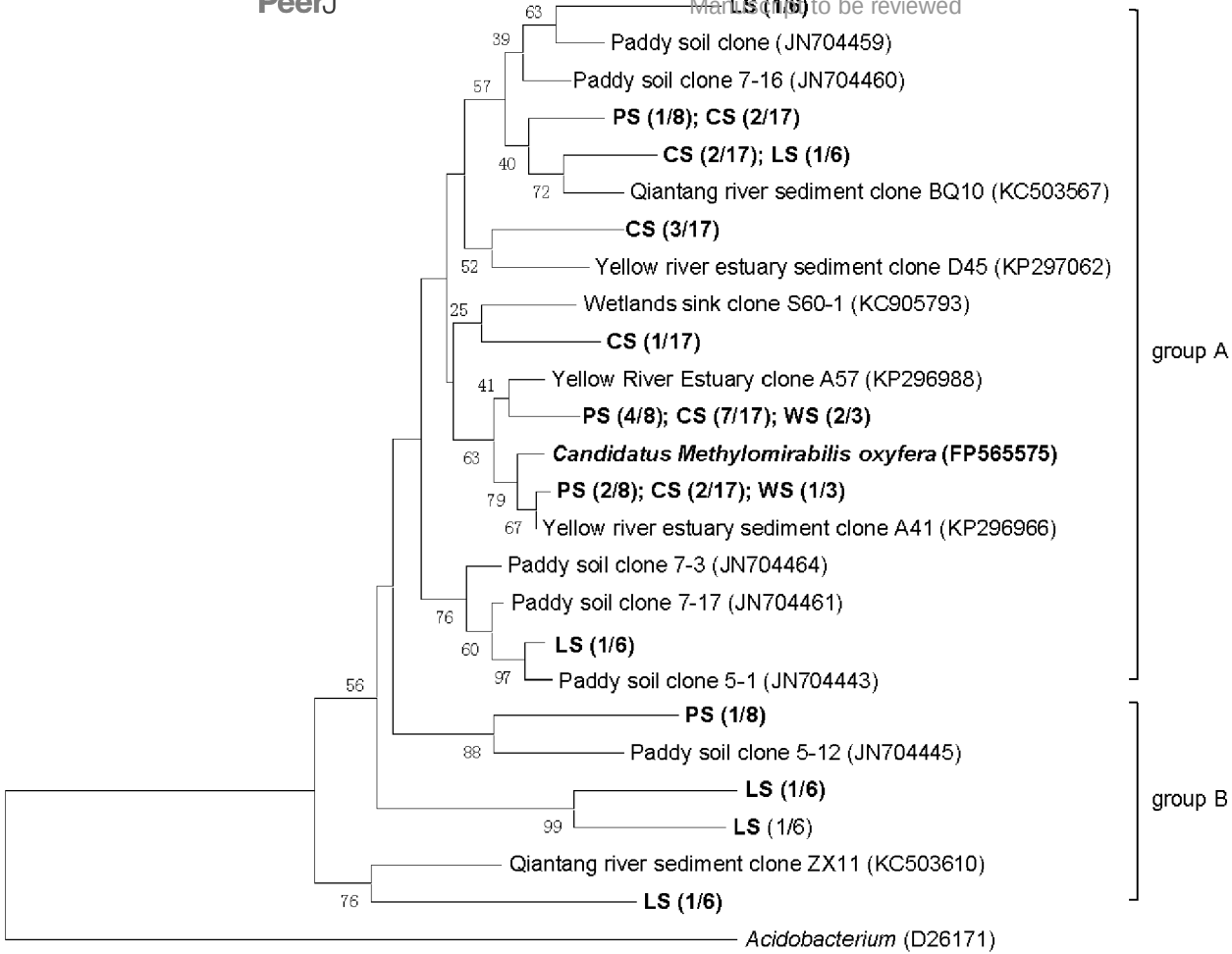
63
LS (1/6)
39
Paddy soil clone (JN704459)
57
Paddy soil clone 7-16 (JN704460)
PS (1/8); CS (2/17)
40
CS (2/17); LS (1/6)
72
Qiantang river sediment clone BQ10 (KC503567)
CS (3/17)
52
Yellow river estuary sediment clone D45 (KP297062)
25
Wetlands sink clone S60-1 (KC905793)
CS (1/17)
41
Yellow River Estuary clone A57 (KP296988)
PS (4/8); CS (7/17); WS (2/3)
63
Candidatus Methylomirabilis oxyfera (FP565575)
79
PS (2/8); CS (2/17); WS (1/3)
67
Yellow river estuary sediment clone A41 (KP296966)
Paddy soil clone 7-3 (JN704464)
76
Paddy soil clone 7-17 (JN704461)
60
LS (1/6)
97
Paddy soil clone 5-1 (JN704443)
group A
56
PS (1/8)
88
Paddy soil clone 5-12 (JN704445)
LS (1/6)
99
LS (1/6)
group B
Qiantang river sediment clone ZX11 (KC503610)
76
LS (1/6)
Acidobacterium (D26171)
0. 02

Figure 5(on next page)

Phylogenetic tree of *M. oxyfera* bacteria *pmoA* gene

Fig. 5 - Neighbor-joining phylogenetic tree showing the phylogenetic affiliations of *M. oxyfera* bacteria *pmoA* gene sequences in four samples. Bootstrap values were 1,000 replicates and the scale bar represents 5% of the sequence divergence.

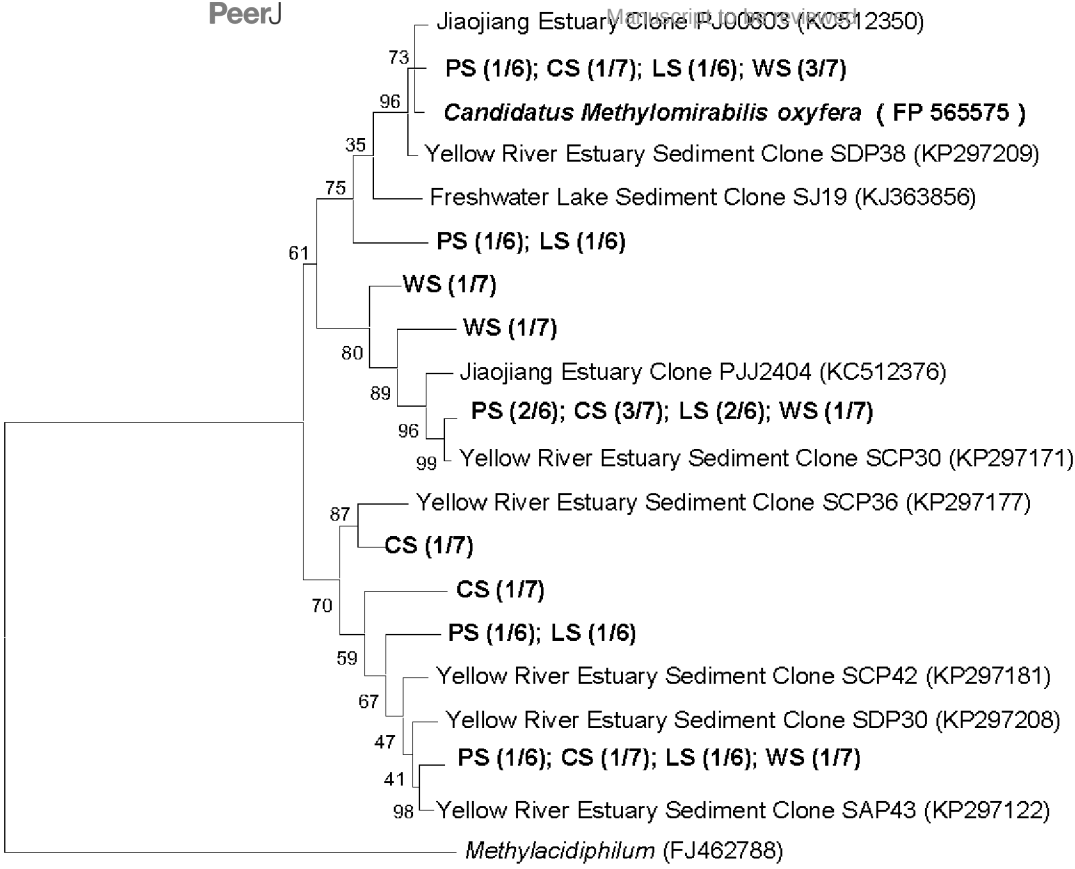
Jiaojiang Estuary Clone PJJ00603 (KC512350)
73
PS (1/6); CS (1/7); LS (1/6); WS (3/7)
96
Candidatus Methylomirabilis oxyfera (FP 565575)
35
Yellow River Estuary Sediment Clone SDP38 (KP297209)
75
Freshwater Lake Sediment Clone SJ19 (KJ363856)
PS (1/6); LS (1/6)
61
WS (1/7)
WS (1/7)
80
Jiaojiang Estuary Clone PJJ2404 (KC512376)
89
PS (2/6); CS (3/7); LS (2/6); WS (1/7)
96
99
Yellow River Estuary Sediment Clone SCP30 (KP297171)
Yellow River Estuary Sediment Clone SCP36 (KP297177)
87
CS (1/7)
CS (1/7)
70
PS (1/6); LS (1/6)
59
Yellow River Estuary Sediment Clone SCP42 (KP297181)
67
Yellow River Estuary Sediment Clone SDP30 (KP297208)
47
PS (1/6); CS (1/7); LS (1/6); WS (1/7)
41
98
Yellow River Estuary Sediment Clone SAP43 (KP297122)
Methylacidiphilum (FJ462788)
0.05